Physics Letters B 759 (2016) 200–205

Contents lists available at ScienceDirect

Physics Letters B

www.elsevier.com/locate/physletb

Coulomb and nuclear excitations of narrow resonances in ^{17}Ne

J. Marganiec [a,b,c], F. Wamers [a,b,c,d], F. Aksouh [b], Yu. Aksyutina [b], H. Álvarez-Pol [e], T. Aumann [a,b], S. Beceiro-Novo [e], C.A. Bertulani [f], K. Boretzky [b], M.J.G. Borge [g], M. Chartier [h], A. Chatillon [b], L.V. Chulkov [i,b], D. Cortina-Gil [e], H. Emling [b], O. Ershova [b,j], L.M. Fraile [k], H.O.U. Fynbo [l], D. Galaviz [g], H. Geissel [b], M. Heil [b], D.H.H. Hoffmann [a], J. Hoffmann [b], H.T. Johansson [m], B. Jonson [m,*], C. Karagiannis [b], O.A. Kiselev [b], J.V. Kratz [n], R. Kulessa [o], N. Kurz [b], C. Langer [b,j], M. Lantz [p], T. Le Bleis [b,q], R. Lemmon [r], Yu.A. Litvinov [b], K. Mahata [b,s], C. Müntz [b], T. Nilsson [m], C. Nociforo [b], G. Nyman [m], W. Ott [b], V. Panin [a,b], S. Paschalis [b,h], A. Perea [g], R. Plag [b,j], R. Reifarth [b,j], A. Richter [a], C. Rodriguez-Tajes [e], D. Rossi [b,u], K. Riisager [l], D. Savran [c,d], G. Schrieder [a], H. Simon [b], J. Stroth [j], K. Sümmerer [b], O. Tengblad [g], S. Typel [b], H. Weick [b], M. Wiescher [t], C. Wimmer [b,j]

[a] *Institut für Kernphysik, Technische Universität Darmstadt, DE-64289 Darmstadt, Germany*
[b] *GSI Helmholtzzentrum für Schwerionenforschung GmbH, DE-64291 Darmstadt, Germany*
[c] *ExtreMe Matter Institute EMMI and Research Division GSI, DE-64291 Darmstadt, Germany*
[d] *Frankfurt Institute for Advanced Studies FIAS, DE-60438 Frankfurt am Main, Germany*
[e] *Departamento de Física de Partículas, Universidade de Santiago de Compostela, ES-15782 Santiago de Compostela, Spain*
[f] *Department of Physics and Astronomy, Texas A&M University-Commerce, TX 75429, USA*
[g] *Instituto de Estructura de la Materia, CSIC, ES-28006 Madrid, Spain*
[h] *Department of Physics, University of Liverpool, Liverpool, L69 3BX, United Kingdom*
[i] *NRC Kurchatov Institute, RU-123182 Moscow, Russia*
[j] *Institut für Angewandte Physik, Goethe Universität, DE-60438 Frankfurt am Main, Germany*
[k] *Department of Atomic, Molecular and Nuclear Physics, Universidad Complutense de Madrid, ES-28040 Marid, Spain*
[l] *Department of Physics and Astronomy, University of Aarhus, DK-8000 Aarhus, Denmark*
[m] *Fysik, Chalmers Tekniska Högskola, SE-412 96 Göteborg, Sweden*
[n] *Institut für Kernchemie, Johannes Gutenberg-Universität Mainz, DE-55122 Mainz, Germany*
[o] *Instytut Fizyki, Uniwersytet Jagelloński, PL-30-059 Krakóv, Poland*
[p] *Institutionen för Fysik och Astronomi, Uppsala Universitet, SE-75120 Uppsala, Sweden*
[q] *Physik-Department E12, Technische Universität München, DE-85748 Garching, Germany*
[r] *Nuclear Physics Group, STFC Daresbury Lab, Warrington, WA4 4AD, Cheshire, UK*
[s] *Nuclear Physics Division, Bhabha Atomic Research Centre, Trombay, Mumbai, 400 085, India*
[t] *JINA, University of Notre Dame, Notre Dame, USA*
[u] *National Superconducting Cyclotron Laboratory, MSU, East Lansing, MI 48824, USA*

ARTICLE INFO

Article history:
Received 16 February 2016
Received in revised form 11 April 2016
Accepted 22 May 2016
Available online 25 May 2016
Editor: V. Metag

ABSTRACT

New experimental data for dissociation of relativistic ^{17}Ne projectiles incident on targets of lead, carbon, and polyethylene targets at GSI are presented. Special attention is paid to the excitation and decay of narrow resonant states in ^{17}Ne. Distributions of internal energy in the $^{15}\mathrm{O}+p+p$ three-body system have been determined together with angular and partial-energy correlations between the decay products in different energy regions. The analysis was done using existing experimental data on ^{17}Ne and its mirror nucleus ^{17}N. The isobaric multiplet mass equation is used for assignment of observed resonances and their spins and parities. A combination of data from the heavy and light targets yielded cross sections and transition probabilities for the Coulomb excitations of the narrow resonant states. The

* Corresponding author.
E-mail address: Bjorn.Jonson@chalmers.se (B. Jonson).

http://dx.doi.org/10.1016/j.physletb.2016.05.073

resulting transition probabilities provide information relevant for a better understanding of the ^{17}Ne structure.

The proton dripline nucleus ^{17}Ne is a candidate for a two-proton Borromean halo nucleus [1], with a ^{15}O core surrounded by two valence protons. The protons are expected to predominantly possess a mixed $(1s_{1/2})^2$ and $(0d_{5/2})^2$ configuration. There is, however, no real consensus about the relative strength of the s and d configurations, neither experimentally nor theoretically. Estimates based on experimental values for interaction cross-section and momentum distributions of fragments in one-proton knockout [2–5], the magnetic dipole moment [6], first-forbidden β^+-decay [7,8], Coulomb energy difference between the mirror nuclei ^{17}Ne and ^{17}N [9–13], as well as pure theoretical investigations [14–16], provide widely differing results. Different evaluations of the amount of $(1s_{1/2})^2$ in the ^{17}Ne ground-state wave function, P(s^2), range from 15% to 100%. There are also strong contradictions between different theoretical models for Coulomb dissociation of ^{17}Ne [17–20].

A theoretical study [21] points to the importance of the determination of electric transition strengths to elucidate the two-proton halo properties. The authors emphasise in particular the importance of reduced electric transition probabilities from the ^{17}Ne ground state to low-lying states as for example $B(E2, 1/2^- \rightarrow 3/2^-)$ and $B(E2, 1/2^- \rightarrow 5/2^-)$, that could be determined through Coulomb excitation.

This paper presents a new comparative study of nuclear and Coulomb excitation of ^{17}Ne at relativistic energies using polyethylene (CH_2), carbon, and lead targets.

The experiment was performed at the GSI Helmholzzentrum für Schwerionenforschung GmbH in Darmstadt, employing the R^{3}B-LAND setup for measurements in inverse and full kinematics. The reaction products, from ^{17}Ne interaction, were first detected in a pair of silicon-strip detectors and then separated in the magnetic field of the large dipole magnet (ALADIN). After the magnet, two branches of detectors were used to measure the position, energy-loss, and time-of-flight, one for heavy ions (two fibre detectors and a ToF-wall) and another for protons (two drift chambers PDC and a ToF-wall). The trajectories of charged particles through the magnetic field of ALADIN were reconstructed for particle identification and determination of their momentum vectors. The charge of the particles was directly measured via their energy loss in the silicon-strip detectors and ToF-walls, while their mass was obtained from measurements of $B\rho$ using the reconstructed deflection angle in the ALADIN magnet. This analysis is based on knowledge of the magnetic field inside and outside the ALADIN magnet, measured along all three coordinate axes at many thousands of grid points. The γ-rays emitted by the de-exciting fragments were detected in the 4π gamma spectrometer, Crystal Ball, placed around the target. A sketch of the positions of the charged-particle detectors in the experimental setup is shown in Fig. 1 of Ref. [22].

The ^{17}Ne beam was directed towards a secondary 199 mg/cm lead target, used to induce electromagnetic excitation of ^{17}Ne. The experiment also took data with a 370 mg/cm^2 carbon target as well as a 213 mg/cm^2 polyethylene target, to study nuclear-induced breakup. The background was determined in runs with an empty target.

Triple coincidences between ^{15}O and two protons were selected. The intrinsic two-proton detection efficiency was 57.8(3.1)%. The detection efficiency was determined from losses of two-proton events due to too small energy deposited in the PDCs, losses during the reconstruction of proton trajectories in the magnetic field of ALADIN, and losses due to the spatial resolution in the PDCs. The losses due to PDC resolution are increasing with the decreasing internal energy in the three-body system. However even at the energy of the ^{17}Ne$(5/2^-)$ resonance the change in the detection efficiency was found to be smaller than its uncertainty. The magnetic spectrometer provided large difference in proton trajectories. Quadruple coincidences, including γ-ray detectors, showed that contributions from excited states in ^{15}O are negligible.

The momentum vectors of the protons and the ^{15}O fragments were obtained in the rest frame of the beam. As in Ref. [22] and its Eq. (1), Jacobi coordinates in the **Y**-system were used in the analysis. The internal kinetic energy, E_{fpp}, in the three-body $^{15}\mathrm{O}+p+p$ system, as well as the fractional energies $\epsilon_{fp} = E_{fp}/E_{fpp}$ in the fragment-proton subsystem and the angle θ_{fp} between the two vectors $\mathbf{p}_{fp}$ and $\mathbf{p}_{p-fp}$, was determined for each event. The analysis was done in two consecutive loops through each event, by selecting one detected proton as the first one in the first loop and then changing to the opposite order in the second loop. The data were corrected for acceptance. The overall acceptance, including momentum cuts due to the finite size of detectors and dead wires in the proton drift chambers, was calculated in a Monte-Carlo simulation under the assumption of isotopic three-body decay. The acceptance function on E_{fpp} is shown in Fig. 3 of Ref. [22]. The experimental energy resolution was found to be close to a Gaussian shape with a dispersion $\sigma = 1.83 E_{fpp}^{0.568}$ MeV.

The correlation functions, for the fractional-energy distributions $W(\epsilon_{fp})$ as well as for the angular distributions $W(\theta_{fp})$, normalised to unity ($\int_0^1 W(\epsilon)\mathrm{d}\epsilon = 1$ and $\int_{-1}^1 W(\theta)\mathrm{dcos}\theta = 1$) were then constructed and analysed.

The experimental excitation energy spectra, $E^* = E_{fpp} + S_{2p}(^{17}\mathrm{Ne})$, shown in Fig. 1, are well described as resulting from the contribution of several excited states in ^{17}Ne, superimposed on a smooth background, shown as dashed lines. This background corresponds to non-resonant dissociation and may also contain contributions from unresolved resonances. Based on experimental results [25], the widths of the resonance structures were assumed as determined entirely by the experimental resolution. A least-squares fit was performed using the functional minimisation and error analysis code MINUIT [24]. The smooth background, shown as dashed lines in Fig. 1, corresponds to non-resonant dissociation and may also contain contributions from unresolved resonances. Extrapolation of this smooth background into the region of resonances was done by using information from the $W(\epsilon_{fp})$ distributions (see Fig. 5).

Five resonance-like structures corresponding to excitations of narrow resonant states in ^{17}Ne are observed in the data from the CH_2 and C targets, while only three are identified in the data from the Pb target (see Fig. 1 and Table 1). The level structure of ^{17}Ne has been studied earlier using the three-neutron transfer reaction ^{20}Ne(^{3}He,^{6}He) [25]. These results were used as a first guidance in our interpretation together with the available experimental information about the structure of excited states in the mirror nucleus ^{17}N [26]. Atomic masses and energy levels of the $A = 17$, $T = 3/2$ isobaric multiplets taken from Refs. [27,28] were also used together with the isobaric multiplet mass equation (IMME) and the Thomas–Ehrman shifts (TESs) for the classification of the states.

(1) The first peak in the spectrum is due to an unresolved doublet consisting of two narrow states at 1.764(12) MeV ($I^\pi = 5/2^-$) and at 1.908(15) MeV ($1/2^+$) [25]. The relative contribu-

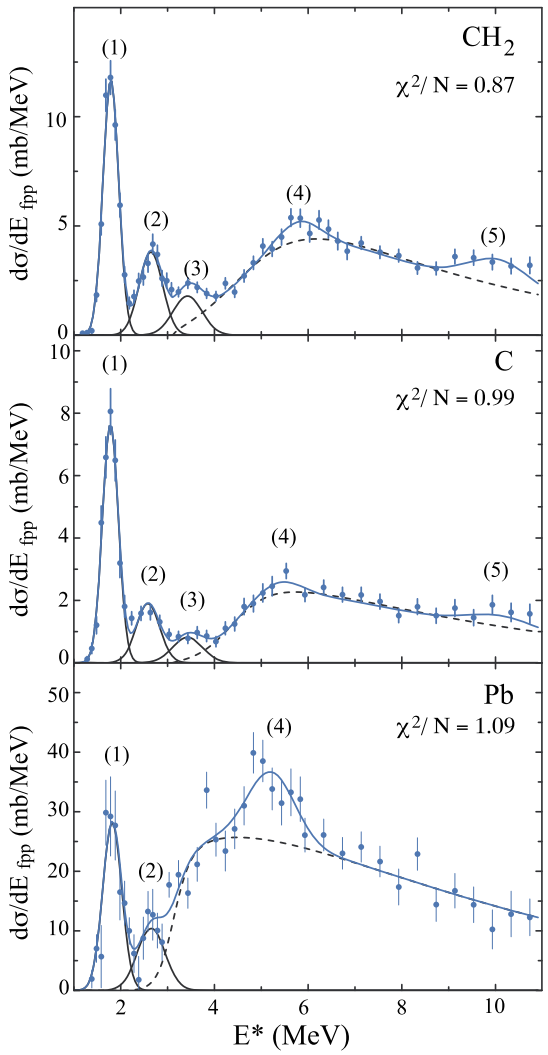

Fig. 1. Excitation spectra of ^{17}Ne after breakup of ^{17}Ne 500 MeV/u beam to ^{15}O + $p + p$ in polyethylene, carbon and lead targets. The numbers in parentheses refer to the resonances presented in Table 1.

tions of these two states were obtained from an analysis of the three-body correlations in the energy region $0 < E_{fpp} < 1.4$ MeV (see below).

(2) The second peak at $E^* = 2.652$ MeV (see Table 1) is close in energy to the observed excited state at 2.651(12) MeV [25]. This state was interpreted to be an $I^\pi = 5/2^+$ state. However, a $5/2^+$ state is unlikely to be fed in a Pb target by Coulomb excitation due to the small strength of the required E3 or M2 transitions. Hence, the possibility that the observed peak is due to an unresolved doublet cannot be excluded. Overlapping states with the spin-parity, $5/2^+_1$ and $5/2^-_2$, were proposed (see Ref. [25] and references therein). However, in this case an unusually large negative cubic-term coefficient is required ($d = -25$ keV) in the isobaric multiplet mass equation (IMME) for the $5/2^-_2$ iso-quartet and furthermore the Thomas–Ehrman shift for the $5/2^-_2$ state is surprisingly large in this case (≈ 1 MeV).[1] An alternative hypothesis is an unresolved doublet of $5/2^+_1$ and $3/2^-_2$ states. The parabolic IMME was used in the analysis (see Table 2). The position of the $T = 3/2$, $I^\pi = 3/2^-_2$ state in ^{17}O is not known, but the assumption of a doublet requires that the positions of the $5/2^+_1$ and $3/2^-_2$ states in ^{17}Ne are close in energy, which only leaves one possibility for this state – a narrow state at 14.230(2) MeV. The fit using only three states from ^{17}N, ^{17}O and ^{17}F allows then to make a prediction for the positions of states: $5/2^+_1$ at 2.614(20) MeV and $3/2^-_2$ at 2.692(21) MeV, respectively. The resulting TES($3/2^-_2$) = 380(16) keV, is much larger than TES($3/2^-_1$) = −47(14) keV. The structure of the analog states in the mirror nucleus ^{17}N has shown that the $3/2^-_1$ and $3/2^-_2$ states have wave functions [26] with a 14% configuration with one valence proton in the s-shell for $3/2^-_1$ and 86% for $3/2^-_2$ [26]. A similar structure is expected for the analog states in ^{17}Ne. Thus a small value for TES($3/2^-_1$) and a large for TES($3/2^-_2$) can be explained as a large asymmetry in the weights of the configuration with one valence nucleon in the s-shell and the large spatial extension of the s-wave proton wave function.[2]

(3) The excitation energy of the third peak, at $E^* = 3.415(38)$ MeV, is close to the observed position of the $9/2^-$ state at $E^* = 3.548(20)$ MeV [25], but the energy difference and the fact that there is no sign of a $7/2^-$ state, which should have similar structure as the $9/2^-$ state [26], excludes such an assign-

Table 2
Isobaric multiplet mass equation coefficients and Thomas–Ehrman shifts (keV), (TES), for $A = 17$, $T = 3/2$ states. See explanations in the text.

I^π	a	b	c	χ^2	TES
$3/2^-_1$	13025(1.2)	−2844.8(1.3)	219.8(3.6)	0.39	−47(14)
$5/2^-_1$	1349(2.5)	−2825.0(3.5)	210.10(4.9)	0.61	20(16)
$1/2^+$	13523(3.8)	−2896.4(4.7)	240.28(5.5)	0.00	−190(19)
Assuming $5/2^+_1$ and $3/2^-_2$ both at E* = 2.651 MeV.					
$5/2^+_1$	14219(2.9)	−2910.5(3.8)	247.9(4.9)	2.4	
$3/2^-_2$	14729(3.2)	−2699.4(4.5)	169.4(5.0)	2.4	
Fit to only ^{17}F, ^{17}O and ^{17}N isobars.					
$5/2^+_1$	14220(3.0)	−2906.2(4.7)	237.8(8.1)	–	−220(23)
$3/2^-_2$	14730(3.2)	−2706.2(6.3)	179.5(8.4)	–	380(16)

[1] The Thomas–Ehrman shift, TES(I^π), was defined as the difference between the distances from $7/2^-$ to I^π states in the mirror nuclei ^{17}Ne and ^{17}N. The $7/2^-$ states were chosen as reference since the Coulomb-energy shifts for these states, having three-body structure with two valence nucleons in the d-shell, are expected to be small.

[2] Note also a large negative TES for positive-parity states. These states cannot be incorporated in the three-body models generally used for the description of ^{17}Ne structure and reactions involving this nucleus. An explanation of the experimental parity-dependence of the Coulomb-energy shifts of the $A = 17$ iso-quartet was suggested, e.g., in Ref. [13], using a model with five valence nucleons around the ^{12}C core.

Table 1
Excitation energies (MeV) and cross sections (mb) with statistical error bars for observed resonance structures in ^{17}Ne excitation spectra. The number N refers to the structures shown in Fig. 1.

N	CH_2		Carbon		Lead	
	E^*	σ	E^*	σ	E^*	σ
(1)	1.790(5)	4.89(15)	1.780(8)	3.25(15)	1.813(15)	14.08(93)
(2)	2.652(10)	2.39(14)	2.571(37)	1.17(10)	2.603(45)	7.68(74)
(3)	3.422(44)	1.38(12)	3.393(78)	0.646(87)	–	–
(4)	5.79(12)	1.13(22)	5.40(20)	0.47(19)	5.210(79)	14.4(1.7)
(5)	10.06(16)	2.10(35)	10.69(59)	0.91(46)	–	–

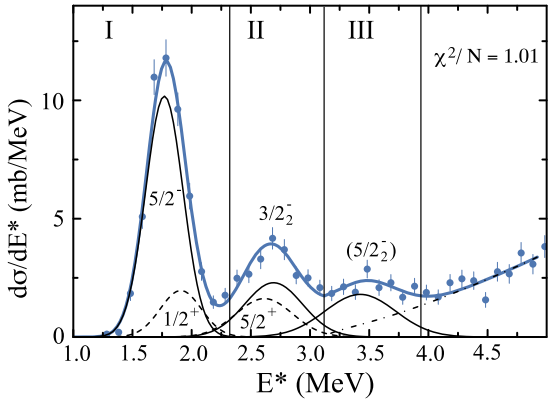

Fig. 2. Narrow resonance states in the low-energy region, $0 < E^* < 4$ MeV excited in the CH_2 target. The thin solid lines show negative-parity states, dashed lines stem for positive-parity states and the dash-dotted line is physical background. For energy regions I, II and III the fractional energy spectra are analysed as shown in Figs. 3, 4 and 5, respectively.

Table 3
Excitation energies and cross sections (mb) with statistical errors for resolved resonances in ^{17}Ne.

I^π	E^*	CH_2	C	H	Pb
$5/2^-$	(i) 1.764(12)	4.04(20)	2.44(18)	0.80(14)	11.6(1.5)
$1/2^+$	(i) 1.908(15)	0.85(15)	0.81(15)	< 0.1	2.5(1.2)
$5/2^+$	2.614(20)	0.97(51)	1.14(10)	< 0.2	7.68(74)
$(3/2^-_2)$	2.692(21)	1.40(53)	< 0.3	0.70(26)	
$(5/2^-_2)$	3.415(38)	1.37(12)	0.62(10)	0.38(8)	–
$(3/2^+)$	5.210(79)	1.13(22)	0.46(19)	0.33(15)	14.4(1.7)

(i) Energies and errors are from Ref. [25].

ment. The ^{17}Ne level scheme is rather intricate, which makes the analysis knotty. The three-neutron transfer reaction has a selectivity to excitation of states with a definite structure and some states may therefore be missed. A comparison with the level scheme of mirror nucleus, ^{17}N, suggests that this state could be the second $5/2^-$ state. The analysis given in Ref. [26] for the $5/2^-_2$ state in ^{17}N, gave a weight of 72% for a configuration with a single proton in the *s*-shell, a structure similar to that of the $3/2^-_2$ state. The present value $\mathrm{TES}(5/2^-_2) = 359(40)$ keV is close to $\mathrm{TES}(3/2^-_2) = 380(16)$ keV and is thus in support of the $5/2^-_2$ assignment for the $E^* = 3.415(38)$ MeV state in ^{17}Ne.

(4)–(5) Two additional resonances at 5.210(79) MeV and 10.06(16) MeV were observed in the present experiment, the latter only for the light targets. A comparison with the levels in the mirror nucleus ^{17}N and the fact that the resonance at 5.210(79) MeV is strongly excited with the lead target, points to an assignment of $I^\pi = 3/2^+$.

The analysis of the narrow resonant states in the low energy region, based on the discussion above, is shown in Fig. 2 and the results are given in Table 3. Cross sections for excitation of energy levels in the ^{1}H(^{17}Ne(g.s.),^{17}Ne(I^π)) reaction were obtained from the relation: $\sigma(CH_2) = \sigma(C) + 2\sigma(H)$. The data demonstrate different selectivity for the different targets. Thus, for the hydrogen target, positive-parity states have lower excitation probability compared to those with negative-parity. The partial decay scheme with dominating decay branches is shown in Fig. 6.

In order to extract more information from the data, the low-energy part of the E_{fpp} spectrum was divided into three separate regions, as show in Fig. 2, where the fractional energy spectrum $W(\epsilon_{fp})$ and the angular distribution $W(\theta_{fp})$ were constructed and analysed. A sequential decay via an intermediate narrow resonance in ^{16}F at $\epsilon_r = E_r/E_{fpp}$ appears in the $W(E_{fp})$ distribution as two peaks at ϵ_r and $1 - \epsilon_r$. A ^{2}He decay, or diproton emission, would

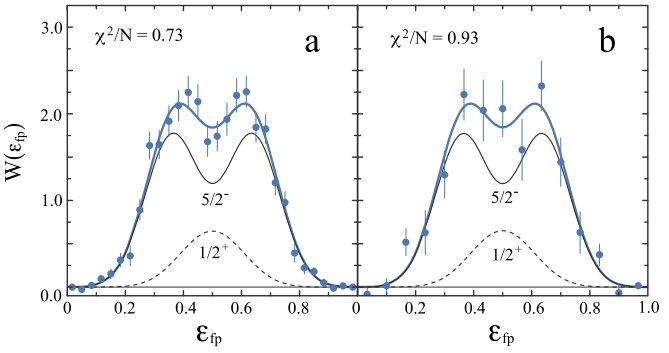

Fig. 3. Fractional energy spectra $W(\epsilon_{fp})$ in the **Y**-system for the region of ^{15}O + $p + p$ internal energy $0 \le E_{fpp} \le 1.4$ MeV from the CH_2 target (a) and Pb target (b). The distributions stem from the unresolved resonances ^{17}Ne($5/2^-$) and ^{17}Ne($1/2^+$) decaying to the ^{16}F ground state. A fit with only one free parameter gives their relative contributions.

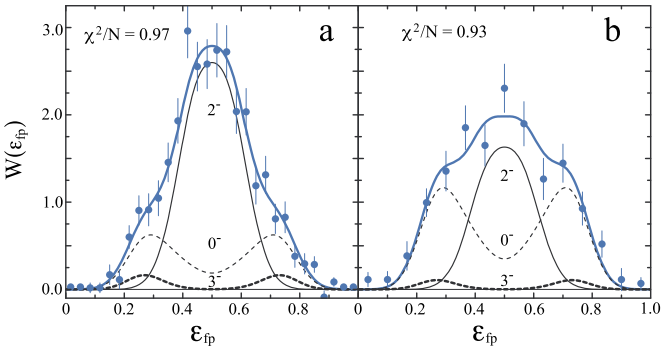

Fig. 4. Fractional energy spectra $W(\epsilon_{fp})$ in the **Y**-system for the region of ^{15}O + $p + p$ internal energy $1.4 \le E_{fpp} \le 2.2$ MeV from the CH_2 target (a) and Pb target (b). Thin solid and thick dashed lines show decays through the intermediate ^{16}F(2^-) and ^{16}F(3^-) states, respectively. These states have the structure of ^{15}O with one proton in the *d*-shell. The dashed lines represent decays to the ^{16}F(0^-) state with the structure ^{15}O with one proton in the *s*-shell.

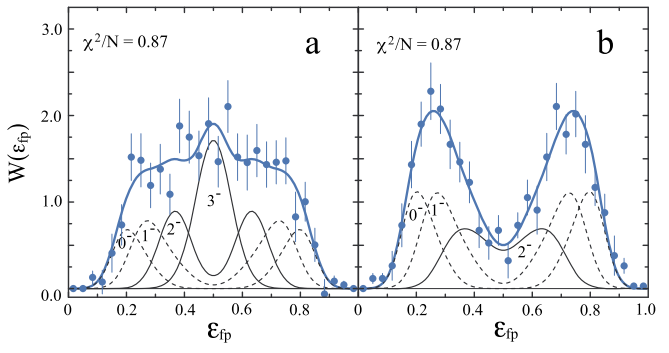

Fig. 5. Fractional energy spectra in the **Y**-system $W(\epsilon_{fp})$ for the region of ^{15}O + $p + p$ internal energy $2.2 \le E_{fpp} \le 3.0$ MeV from the CH_2 target (a) and Pb target (b). The thin solid lines show decays to ^{16}F(2^- and 3^-) states and the dashed lines represent decays to ^{16}F(0^- and 1^-) states.

be characterised by an asymmetric angular $W(\theta_{fp})$ distribution, increasing when θ_{fp} gets close to 180°. In the present analysis $W(\theta_{fp})$ was found to be close to isotropic, within statistical uncertainties, which excludes a significant ^{2}He emission. The shapes of the $W(\epsilon_{fp})$ distributions are well described by assuming sequential decays through the first four excited states in ^{16}F. The parameters for these states were taken from Ref. [23]. The partial $W(\epsilon_{fp})$ shapes are strongly influenced by the experimental resolution and were calculated in Monte-Carlo simulations. The MINUIT

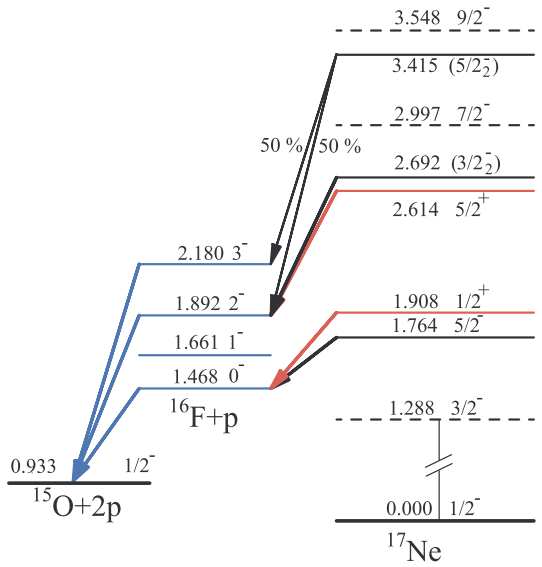

Fig. 6. Narrow resonance states above the two-proton separation energy in ^{17}Ne. The dominant decay branches of the resonant states to $^{15}O + 2p$, via intermediate resonant states in ^{16}F, are shown. Positive-parity states are coloured in red online. Resonances shown as dashed lines are from Ref. [25] and are not populated in the present experiment.

code was used for the least-square fits to the measured $W(\epsilon_{fp})$ spectra.

The fractional energy spectra for the lowest energy bin, $0 \leq E_{fpp} \leq 1.4$ MeV, are shown in Fig. 3. The panels (a) and (b) show least-square fits to the $W(\epsilon_{fp})$ distributions assuming sequential decay from states at excitation energies 1.764 MeV $(5/2^-)$ and 1.908 MeV $(1/2^+)$ [25] through the intermediate ^{16}F(0^-) state. The distributions $W(\epsilon_{fp})$ are normalised to unity and in the fit the relative intensity was the only free parameter used. For the CH_2 target the fit gives a 17.5(3.2)% contribution from the $1/2^+$ decay, for C 25.0(4.3)% (not shown), and for Pb 17.6(8.7)%, with statistical errors.

A doublet with $5/2^+$ and $3/2^-_2$ states was identified in the energy region $1.4 \leq E_{fpp} \leq 2.2$ MeV (region II in Fig. 2). The difference in excitation energy of these two states is much smaller than the experimental resolution and the difference in shape of $W(\epsilon_{fp})$ for the decay branches is marginal. The penetrability through the Coulomb and centrifugal barriers for the decay of $5/2^+$ to 3^- is about 20 times smaller than that for the decay to the 2^- state. Further, this ratio is around 1000 for the decay of $3/2^-_2$ state. The main decay branches for both states are therefore expected to proceed via the ^{16}F(2^-) state. The analysis of $W(\epsilon_{fp})$ from a carbon target gave a decay branch of 86(2)% while the rest can be attributed to the feeding of the ^{16}F(3^-) state. The $W(\epsilon_{fp})$ from CH_2 and Pb targets were fitted with an assumption that the ^{17}Ne$(5/2^+)$ and ^{17}Ne$(3/2^-_2)$ states decay predominantly through ^{16}F(2^-) and ^{16}F(0^-) states. Contributions from the ^{16}F(2^-) branch were 74(2)% for CH_2 and 41(4)% for Pb targets, see Fig. 4. The rest can be attributed to feeding mainly of the ^{16}F(0^-) state with a small contribution from the ^{16}F(3^-) branch. In the case of the Pb target, the main part of the ^{16}F(0^-) branch is coming from a continuous E_{fpp} spectrum.

In the energy region $2.2 \leq E_{fpp} \leq 3.0$ MeV a contribution from the ^{17}Ne$(5/2^-_2)$ state is expected. The decay branches from this resonance should proceed mainly by emission of $\ell = 0$ protons, feeding dominantly 2^- and 3^- states in ^{16}F. The population of 0^- and 1^- states in the resonance decay requires emission of $\ell = 2$ protons and is expected to be small due to penetrability factors. Still there are sizeable contributions in the $W(\epsilon_{fp})$ distribution from feeding to these states, especially pronounced for the Pb target, as shown in Fig. 5. These parts of the distributions were treated as a physical background.

The ratio between the feedings $\sigma(2^-)/\sigma(3^-) \approx 1$ was obtained for both the CH_2 and the C target. For the Pb target, keeping this ratio fixed, the $W(\epsilon_{fp})$ cannot be reproduced, which shows that these events cannot be considered as having their origin in the decay of the $5/2^-_2$ state. They were therefore also considered as coming from a continuous E_{fpp} spectrum. The distribution was well fitted with only three decay branched to the 0^-, 1^- and 2^- states in ^{16}F.

The cross sections for Coulomb excitation of resonant states, σ_C, were obtained by subtracting the nuclear contribution from the cross sections measured with the lead target scaled with a factor 1.84(20). The scaling factor was determined experimentally. It was assumed that Coulomb dissociation to ^{14}O has a very small, if not zero, cross section and the scaling factor was determined as the ratio of (^{17}Ne,^{14}O) cross sections obtained with Pb and C targets. The scaling factor is close to the ratio between nuclear radii of projectile and target, $(A_{Ne}^{1/3} + A_{Pb}^{1/3})/(A_{Ne}^{1/3} + A_{C}^{1/3})$, reflecting that the nuclear disintegration is of surface character. In this analysis it was assumed that the $5/2^+$ state is not Coulomb excited. Excitation of this state with a large cross section by a M2 or E3 transition or in a multi-step process is unlikely. Cross sections for Coulomb excitation of the identified narrow resonances are given in Table 1. For the state at $E^* = 5.210(79)$ MeV and a lead target the excitation stems dominantly from Coulomb interaction.

The transition probabilities $B(\pi\lambda)$ from the ground to an excited state in the projectile, where $\pi = E$ or M stands for an electric or magnetic transition with multipolarity λ, were calculated by the virtual-photon method for intermediate energies [29, 30]. The cross section for Coulomb excitation of a narrow resonance at E^* is

$$\sigma_C^{\pi\lambda}(E^*) = \frac{(2\pi)^3(\lambda+1)}{\lambda[(2\lambda+1)!!]^2}\left(\frac{E^*}{\hbar c}\right)^{2\lambda-1}\frac{N(\pi\lambda)}{E^*}B(\pi\lambda), \qquad (1)$$

where $N(\pi\lambda)$ is the number of virtual photons at excitation energy E^*. This expression is used to calculate the transition probability based on the measured cross section $\sigma_C^{\pi\lambda}(E^*)$ (in fm^2).

The formalism described in Refs. [29,30] is used to calculate $N(\pi\lambda)$. In Ref. [30] the effect of strong absorption is incorporated from the outset (see Eqs. (13)–(15)), while a minimal impact parameter B_{cut} has to be used when the analytical semi-classical method from Ref. [29] (Eqs. (2.5.5)) is applied. Calculations using the semi-classical method with $B_{cut} = 10.8$ fm give the same result as Eqs. (13)–(15) in Ref. [30]. The resulting $N(\pi\lambda)$ and $B(\pi\lambda)$ values are given in Table 4.

The Coulomb excitation of the first two excited states in ^{17}Ne was studied earlier [31] and the transition probability $B(E2, 1/2^- \rightarrow 5/2^-) = 24$ e^2 fm^4 was deduced. However, in the $B(E2)$ calculations the authors included an extra factor e^2 in Eq. (1), which means that the obtained $B(E2)$ values are in units of fm^4 and should thus be multiplied with a factor 1.44. The corrected value for $B(E2, 1/2^- \rightarrow 5/2^-)$ is given in the last row in Table 4.

The $B(E2)$ values from Ref. [31] without this correction factor were, however, used in Refs. [21,32] as a confirmation of the proposed ^{17}Ne wave function. The corrected value $B(E2, 1/2^- \rightarrow 5/2^-)$ is about twice larger than that obtained in the present experiment. This might be connected with the assumption, made in Ref. [31], that the detected events were from pure Coulomb excitation. In the present experiment it is shown that nuclear excitation contributes to the cross section with about 50%, see Tables 3 and 4.

Table 4
Coulomb excitation cross sections, σ_C, in mb, for narrow resonant states in ^{17}Ne, virtual-photon numbers and transition probabilities B($\pi\lambda$) in (e^2 $fm^{2\lambda}$). The lowest row gives B($E2$) for $5/2^-$ resonance calculated with Eq. (1) using σ_C and N($E2$) from Table I in Ref. [31].

I^π	E^*	σ_C	$\pi\lambda$	N($\pi\lambda$)	B($\pi\lambda$)
$5/2^-$	1.764	7.13(1.5)	$E2$	11868	90(18)
$1/2^+$	1.908	<2.4	$E1$	121.43	<0.007
$(3/2^-_2)$	2.692	5.57(76)	$E2$	5180.4	69(10)
$(3/2^+)$	5.141	13.6(1.7)	$E1$	68.68	0.071(9)
$5/2^-$	1.764	29.9(4.4)	$E2$	24990	179(26)

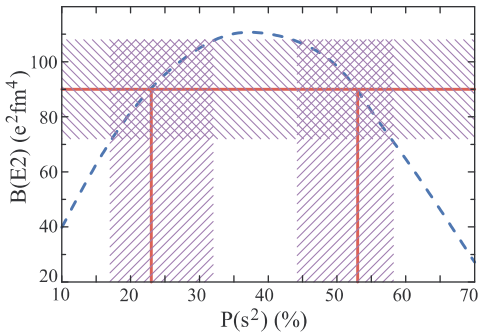

Fig. 7. Transition probabilities $B(E2, 1/2^- \to 5/2^-)$ as a function of the s-shell occupation, $P(s^2)$, in ^{17}Ne(g.s.). The solid line gives experimental $B(E2)$ value and the hatched zone shows the 1σ deviation from this value. The dashed line represents calculations from Ref. [21].

A comparison between the $B(E2, 1/2^- \to 5/2^-)$ values deduced from the present experiment and theoretical calculations from [21] is shown in Fig. 7. The most probable value for the s^2 occupancy would be either $P(s^2) = 23\%$ or $P(s^2) = 53\%$. The hatched zones in Fig. 7 show the 1σ deviations from these values.

In conclusion, new experimental data on dissociation of ^{17}Ne into $^{15}O + 2p$ studied at GSI with a relativistic ^{17}Ne beam impinging on lead, carbon, and polyethylene targets are presented. The main attention is paid to the excitation and decay of narrow resonant states in ^{17}Ne, for which cross sections were measured. Three-body correlations were used to determine the relative contributions to unresolved resonances. The data obtained from lead and carbon targets allowed the determination of cross sections and transition probabilities for Coulomb excitation. The reduced electric quadrupole transition probability B(E2, $1/2^- \to 5/2^-$) = 90(18) e^2 fm^4 was derived by using the virtual-photon method. The measured B(E2) value was compared to the model calculations. Finally, the observation of a resonance at $E^* = 5.210(79)$ MeV tentatively interpreted as $3/2^+$ state, mainly Coulomb excited, is of special interest and should be a subject of further investigations. The excitation of positive parity states implies that three-body models without inclusion of the core intrinsic structure are not able to fully describe the reaction mechanism. Theoretical methods are urgently needed to describe excitation spectra and reaction mechanisms, including techniques beyond three-body models.

Acknowledgements

This project is supported by NAVI, GSI-TU Darmstadt cooperation, HIC for FAIR, EMMI and BMBF. C.A.B. acknowledges support from the U.S. NSF Grant No. 1415655, and U.S. DOE grant No. DE-FG02-08ER41533. The work was also supported by the Spanish government grant FPA2012-32443 and the Swedish Research Council.

References

[1] M.V. Zhukov, I.J. Thompson, Phys. Rev. C 52 (1995) 3505.
[2] A. Ozawa, et al., Phys. Lett. B 334 (1994) 18.
[3] H. Kitagawa, N. Tajima, H. Sagawa, Z. Phys. A 358 (1997) 381.
[4] R. Kanungo, M. Chiba, S. Adhikari, et al., Phys. Lett. B 571 (2003) 21.
[5] K. Tanaka, M. Fukuda, M. Mihara, et al., Phys. Rev. C 82 (2010) 044309.
[6] W. Geithner, et al., Phys. Rev. C 71 (2005) 064319.
[7] M.J.G. Borge, et al., Phys. Lett. B 317 (1993) 25.
[8] J.D. Millener, Phys. Rev. C 55 (1997) R1633.
[9] H.T. Fortune, R. Sherr, Phys. Lett. B 503 (2001) 70.
[10] H.T. Fortune, R. Sherr, B.A. Brown, Phys. Rev. C 73 (2006) 064310.
[11] L.V. Grigorenko, I.G. Mukha, M.V. Zhukov, Nucl. Phys. A 713 (2003) 372; L.V. Grigorenko, I.G. Mukha, M.V. Zhukov, Nucl. Phys. A 740 (2004) 401 (Erratum).
[12] E. Garrido, D.V. Fedorov, A.S. Jensen, Phys. Rev. C 69 (2004) 024002.
[13] S. Nakamura, V. Guimarães, S. Kubono, Phys. Lett. B 416 (1998) 1.
[14] S.S. Zhang, et al., Eur. Phys. J. A 49 (2013) 77.
[15] N.K. Timofeyuk, P. Descouvement, D. Baye, Nucl. Phys. A 600 (1996) 1.
[16] T. Oishi, K. Hagino, H. Sagawa, Phys. Rev. C 82 (2010) 024315; T. Oishi, K. Hagino, H. Sagawa, Phys. Rev. C 82 (2010) 069901 (Erratum).
[17] L.V. Grigorenko, et al., Phys. Lett. B 641 (2006) 254.
[18] T. Oishi, K. Hagino, H. Sagawa, Phys. Rev. C 84 (2011) 057301.
[19] Z.Y. Ma, Y. Tian, Sci. China 54 (2011) 49.
[20] H.L. Ma, et al., Phys. Rev. C 85 (2012) 044307.
[21] L.V. Grigorenko, Yu.L. Parfenova, M. Zhukov, Phys. Rev. C 71 (2005) 051604.
[22] J. Marganiec, et al., Eur. Phys. J. A 51 (2015) 9.
[23] I. Stefan, et al., Phys. Rev. C 90 (2014) 014307.
[24] F. James, M. Roos, Comput. Phys. Commun. 10 (1975) 343.
[25] V. Guimarães, et al., Phys. Rev. C 58 (1998) 116.
[26] H.T. Fortune, et al., Phys. Rev. C 20 (1979) 1228.
[27] M. Wang, et al., Chin. Phys. C 36 (2012) 1603.
[28] TUNL nuclear data evaluations, http://www.tunl.duke.edu/nucldata/.
[29] C.A. Bertulani, G. Baur, Phys. Rep. 163 (1988) 299.
[30] C.A. Bertulani, A.M. Nathan, Nucl. Phys. A 554 (1993) 158.
[31] M.J. Chromik, et al., Phys. Rev. C 66 (2002) 024313.
[32] W. Geithner, et al., Phys. Rev. Lett. 101 (2008) 252502.